

Lasers in Manufacturing Conference 2019

Design, manufacturing and test of a highly dynamic piezo-driven metal mirror for laser material processing

P. Böttner^{a*}, C. Reinlein^a, A. Jahn^b, P. Herwig^b, C. Goppold^b, D. Stoffel^c, M. Bach^c

^aFraunhofer Institute for Applied Optics and Precision Engineering IOF Albert-Einstein-Straße 7, 07745 Jena, Germany

^bFraunhofer Institute for Material and Beam Technology IWS, Winterbergstrasse 28, 01277 Dresden, Germany

^cPhysik Instrumente (PI) GmbH & Co. KG, Auf der Roemerstrasse 1, 76228 Karlsruhe, Germany

Abstract

This paper reports on the opto-mechanical design and manufacturing of a highly dynamic piezo-driven metal mirror. This metal mirror replaces the last 90° deflecting mirror in conventional laser material processing heads. The central element of the mirror is a diamond turned free-form membrane. The membrane design is optimized to correct astigmatic aberrations which arise from the 90° beam deflection while simultaneously shifting the laser focus over a large range. In combination with a 200 mm focus lens, this allows diffraction-limited focus movements of up to 20 mm. A coating is applied to the mirror surface which has been successfully tested for cw laser loads up to 4 kW. The mirror is activated by a controlled piezoelectric stack actuator allowing beam oscillations up to 2.5 kilohertz. Optical, static and dynamic properties of a prototype mirror are characterized in order to qualify the mirror for laser cutting and welding processes.

Keywords: focus shifting; material processing; highly dynamic beam oscillation; aberration correction

1. Introduction

Laser material processing using a highly dynamic deformable mirror that quickly adapts the focus of the laser system is expected to enable both (i) an increase in processing speed [Steen et al., 1980] and (ii) an improvement in the machining quality [Geiger et al., 1996 or Okada et al., 2000 or Morimoto et al., 2015]. Both can be realized due to the faster dynamic behavior of deformable mirrors compared to conventional solutions where lens are shifted or pneumatically actuated deformable mirrors are used [Kugler GmbH, 2019 and SCANLAB GmbH, 2019]. Here, we describe a focusing mirror which is deformed by a piezoelectric stack actuator acting orthogonally to the mirror membrane.

For a user-friendly and compact integration into existing laser beam machining heads, the deformable mirror should be integrated as a 90° deflecting mirror. Additionally, for best machining results, large active

* Corresponding author. Tel.: +49-3641-807-738;
E-mail address: paul.boettner@iof.fraunhofer.de.

refocusing ranges and oscillation frequencies up to 2.5 kHz are favoured. Those requirements result in the need for a very stiff connection of the deformable mirror membrane to the housing. Moreover, the deformable mirror design has to be able to correct the astigmatism which is induced through the reflection on a curved mirror under an angle. This astigmatism can be corrected through a biconic mirror design which allows for variable radii of curvature in the x and y axes. This in turn, can be implemented with a single actuator through the use of an elliptical shaped mirror membrane, the vertex lengths of which are directly related to the individual radii of curvature in x and y.

In section 2 of this paper, we introduce the working principle of the laser machining head and the deformable mirror. In section 3, we give details on the design of the mirror membrane. Section 4 briefly summarizes the manufacturing and integration of the mirror surface. Finally, in section 5, we report the results of the characterization of the mirror surface quality, the active deformation capability, and the dynamic capability of the mirror.

2. Working principle

A collimated beam is reflected on a deformable mirror and then focused by the focal lens. The schematic design is shown in Fig. 1. If the deformable mirror is plane, the focal point of the mirror-lens system is at the nominal focal distance of the focal lens. However, when the deformable mirror is not plane, but convex, it induces a divergence in the beam which shifts the focus of the mirror-lens-system away from the nominal focal distance. The working range of the mirror-lens-system is defined by the capability of the deformable mirror to actively change its radius of curvature, and hence the divergence of the incident beam.

A schematic view of the deformable mirror is shown in Fig. 1. The deformable mirror has a mirror membrane that is deformed by an actuator. Here, a pre-stressed piezoelectric stack actuator [PI Ceramic GmbH, 2019] induces a voltage-dependent centric displacement at the mirror membrane. Thanks to the rim fixation of the mirror membrane, a toric deformation is established that expands the collimated beam and corrects the astigmatic aberration (see Fig. 1).

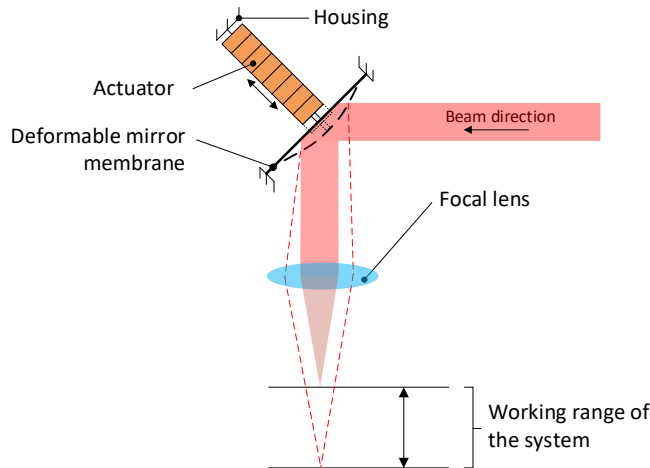


Fig. 1. Working principle and main mechanical components of the deformable mirror.

3. Design of the mirror surface

As has been mentioned, reflection on a spherically curved mirror under an angle results in astigmatism and an elongated spot in the working plane. This arises as depending on the cross-sectional orientation of the light on the mirror surface, the divergence varies. The mirror must have a biconical shape in order to correct this induced astigmatism. Thereby, the resulting divergence will be independent of the cross-sectional beam orientation, resulting in a symmetrical corrected focal point in the working plane. This special surface shape allows for the adjustment of the defocus and the compensation of the astigmatic aberration in a single optical element. Therewith, different radii in the x and y axes are required and are defined by the reflection angle of the mirror. The graph in Fig. 2 shows the ratio of the radii of curvature (R_x/R_y) with respect to deflection angle, necessary to generate a diffraction-limited spot. With increasing deflection angle, the ratio of the radii of curvature grows. A ratio of 2 is necessary for a 90° deflection. The ratio increases rapidly for larger deflection angles. For small deflection angles, the ratio converges at 1 and a biconic design is not essential.

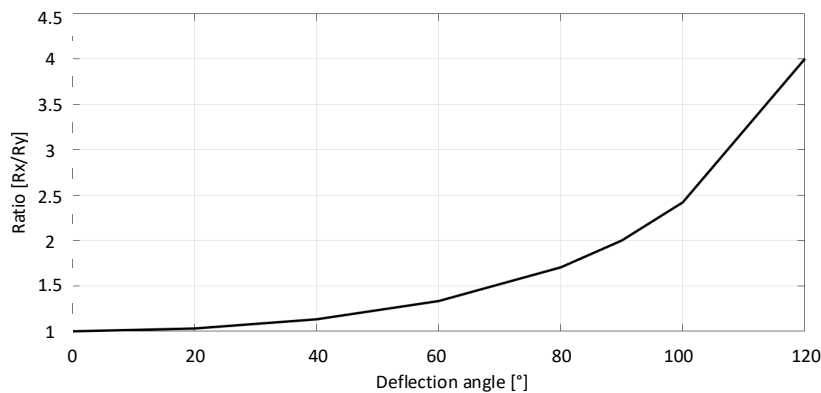


Fig. 2. Ratio of the radii of curvature for the x and y axes with respect to deflection angle.

In Lemaitre, 2008 a variable thickness distribution of the mirror membrane rear surface is suggested for production of a spherical metal mirror under a 0° deflection angle. This variable thickness distribution is taken as a starting point for the development of a mirror membrane which enables different

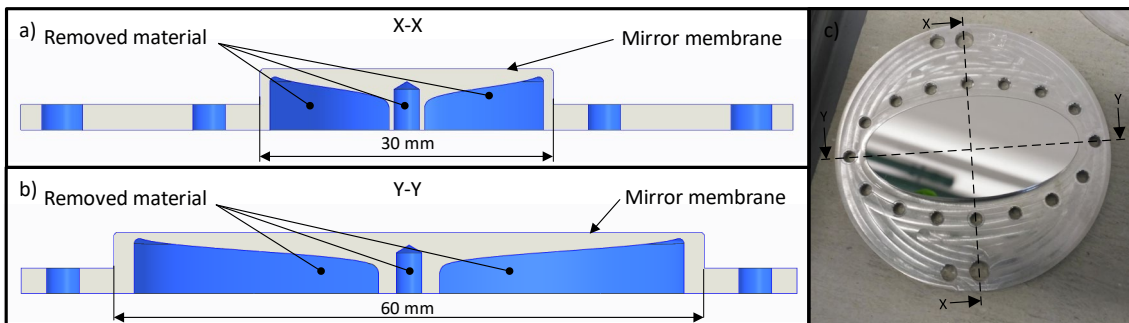


Fig. 3. Cross-sectional views of the mechanical design of the mirror membrane for the X-X axis (a) and Y-Y axis (b) showing the varying thickness profile on the back of the surface. The mirror membrane after manufacturing (c) with an elliptical surface.

radii of curvature in orthogonal axes. The resulting optimized design based on our application is shown in Fig. 3(a) and (b).

4. Manufacturing of the mirror membrane

As material for the manufacturing of the mirror membrane is used RSA6061 based on its good manufacturability, availability and thermal properties. Fig. 3(c) shows the manufactured mirror, and Fig. 3(a) and (b) show the two cross-sectional views that characterize the elliptical mirror. The gray area indicates the mirror substrate while the regions in blue show the material that was removed by conventional turning. A diamond turning process was adapted and successfully realized to finish the mirror surface. Then, a highly reflective high-performance coating is applied to the diamond turned mirror, to enable its application for laser powers up to 4 kW.

In the next step, the mirror membrane is integrated into the housing. To increase the stiffness of the overall system, the mirror membrane is bolted to the housing. Afterwards, a long screw is inserted from the rear of the housing, clamping the actuator between the membrane and housing. With that, the preloading of the actuator is also ensured.

5. Characterization results of the mirror membrane

Characterization of the mirror module includes measurement of the mirror's optical surface as manufactured, evaluation of the static actuation capability through measurement of the actuator influence function, specification of the dynamic actuation capability through determination of the mirror's eigenfrequencies as well as authentication of the high power suitability of the coating, through measurement of the reflected laser power up to 4kW.

5.1. *Performance of the optical surface*

The optical quality of the surface is determined using interferometer. The measurements have shown that surface shape deviations of less than 1 μm peak-to-valley and 200 nm root-mean-square are achieved for the entire membrane after diamond turning (Fig. 4(a)). The illuminated aperture that shall be used in the application is half the size of the physical aperture (Fig. 4(b)). It is standard to design deformable mirror substrates with significantly larger physical apertures as compared to the optical aperture in order to reduce the edge effects on the actuator influence function due to clamping. Within the designed optical aperture, the surface error falls to below 200 nm peak-to-valley and 40 nm root-mean-square (Fig. 4(b)). The evaluation of the surface roughness measurement shows an average roughness of less than 4 nm (Fig. 4(c)). The torsion grooves after diamond turning are evident.

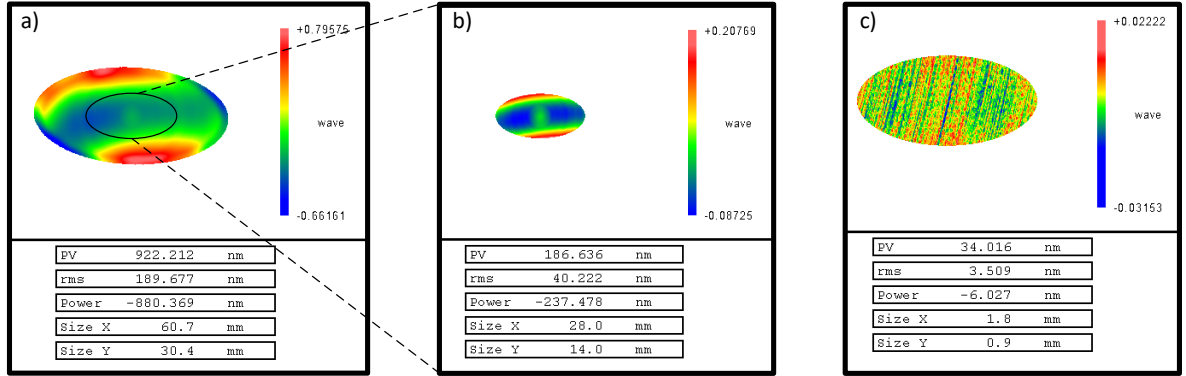


Fig. 4. Optical performance of the mirror membrane: surface shape deviation of the entire aperture (a), the optical aperture (b) and surface roughness of the entire aperture (c).

5.2. Actuator influence function (AIF)

The AIF is defined as the difference between the mirror shape with and without piezoelectric activation. It is obtained by measuring the wavefront reflected by the deformable mirror. The radii of curvature R_x and R_y were determined from a Zernike analysis of the measured wavefront. Fig. 5 (a) presents the measurement results of R_x and R_y over the applied voltage on the deformable mirror. The mirror surface remains flat for low voltages and large R_x and R_y values are measured. With increasing voltage, curvature increases and smaller absolute values of the radii of curvature are measured. These values are plotted as ratios in Fig. 5 (b). It can be seen that the desired ratio of 2 is achieved from a voltage of 400 V and above. Below 300 V, deformation is very small resulting in measurement of large radii of curvature of the nearly flat surface. This accounts for the deviation in the ratio R_x/R_y . The minimal measured radii of curvature are 3 m in the X-

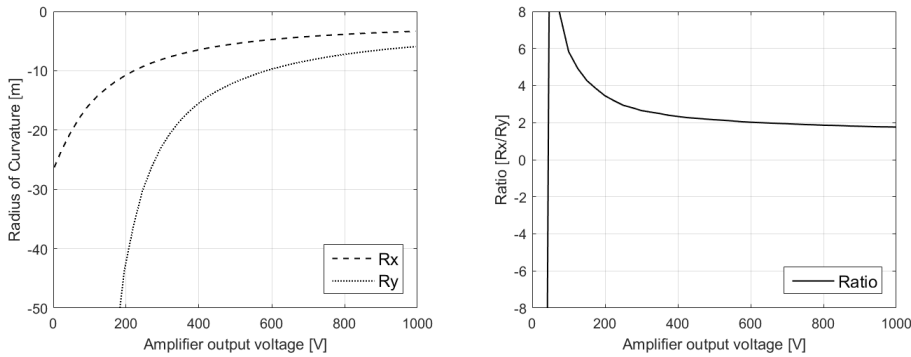


Fig. 5. Mechanical design of the mirror membrane. Cross sections X-X (a) and Y-Y (b). Mirror membrane after manufacturing (c).

direction and 6 m in the Y-direction, or a combined working radius of 4.2 m. The maximum deflection was 28 μm which matches the design values very well. In conjunction with a focal lens, this defines the working range of the system. Combination with a lens of focal length 200 mm provides a maximum shift of the focal spot of 20 mm.

5.3. Eigenfrequencies of the mirror

The eigenfrequencies of the mirror are determined using a vibrometer. It is measured with an actuation voltage of 50 V. The measurement takes place as a surface scan with discrete measuring points on the mirror surface.

The Bode plot in Fig. 6 shows a flat curve between 200 Hz and 8 kHz. The amplitude then steeply increases. The first measured eigenfrequency is at 9.7 kHz and is apparent through a phase jump from -180° to 180° . This is an impressive measurement that qualifies fast step responses and oscillation frequencies of the deformable mirror.

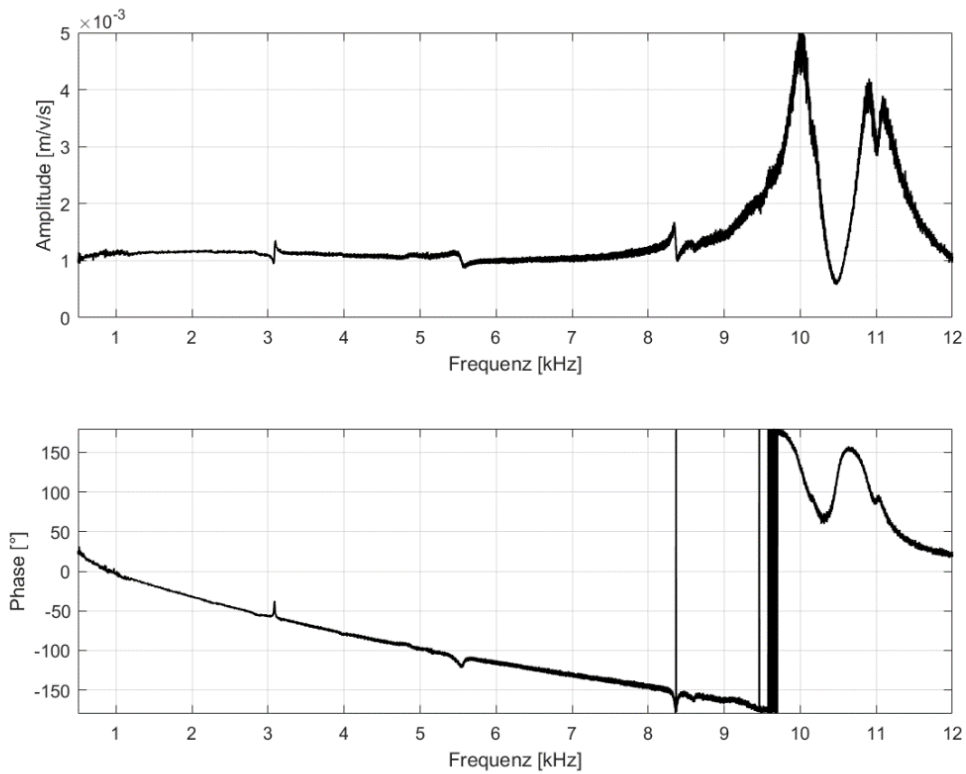


Fig 3. Bode plot of the measured eigenfrequencies of the mirror.

5.4. High power stability

To evaluate the high-power stability, the mirror is compared with a conventional laser cutting head as reference. For this measurement, the deformable mirror is integrated into a laser cutting head under a 90° deflection angle. The actuator of the deformable mirror is not actively controlled. The laser power is gradually increased up to 4 kW and the reflected output laser power is measured. The results are compared with the identical measurements for a conventional laser cutting head setup. They indicate whether the surface condition and coating of the deformable mirror membrane is sufficient for high power laser applications, such as laser beam cutting and welding.

The graphs in Fig. 7 show the output laser power (OUT) over the incident laser power (IN) for the reference (circles) and the deformable mirror (crosses). The comparison reveals an almost identical behavior between the two setups. This measurement verifies the high-power stability of the deformable mirror up to 4 kW in a 90° mounting position.

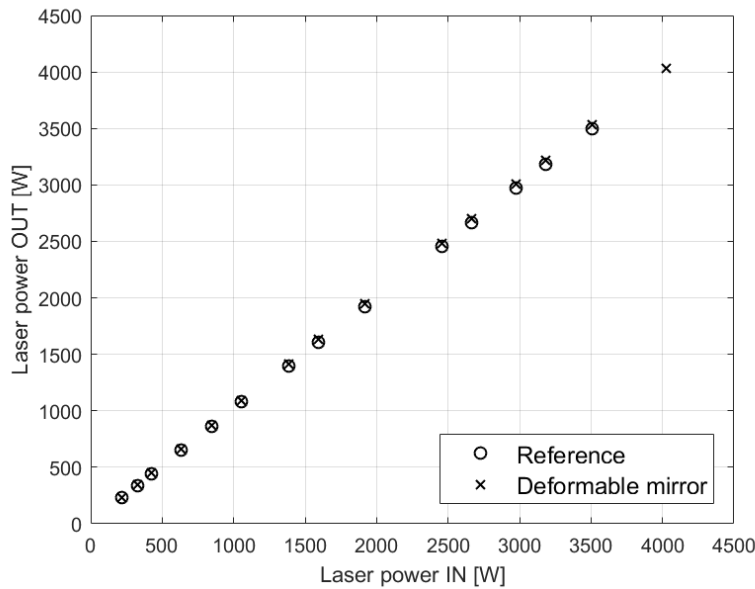


Fig. 4. Input and output laser power to test the high-power stability of the deformable mirror.

6. Summary and outlook

In summary, the present publication reports the working principle and the design of a deformable mirror in a 90° deflection laser machining head. The presented design offers a maximum peak-to-valley deflection of the mirror membrane under piezoelectric activation of $28\ \mu\text{m}$. In conjunction with a focal lens of 200 mm focal length, this enables a working range of the system of 20 mm. Both the designed membrane and actuator allow for oscillation frequencies up to 8 kHz. With that, faster laser machining processes can be initiated in further investigations.

Acknowledgements

The authors are grateful for the financial support given by the Federal Ministry of Education and Research within the project “Piezoangetriebene Strahlformung zur hochdynamischen Lasermaterialbearbeitung im 3D-Raum” as part of the smart³ Innovation Network, Code No: 03ZZ1028F

References

- Steen, William M., 1980. Arc augmented laser processing of materials, *Journal of Applied Physics* 51, p. 5636.
- Geiger, M., Schuberth, S., Hutfless, J., 1996, CO₂ laser beam sawing of thick sheet metal with adaptive optics, *Welding in the World* 37, p. 5.
- Okada, T., Ebata, K., Shiozaki, M., Kyotani, T., Tsuboi, A., Sawada, M., Fukushima, H., 2000. “Development of adaptive mirror for CO₂ laser,” *Proc. SPIE Vol.3888*, Osaka, Japan, pp.509.
- Morimoto, Y., He, D., Hijikata, W., Shinshi, T., Nakai, T., Nakamura, N., 2015. Effect of high-frequency orbital and vertical oscillations of the laser focus position on the quality of the cut surface in a thick plate by laserbeam machining, *Precision Engineering* 40, p. 112.
- Kugler GmbH, 2019; [https://www.kugler-precision.com/index.php?Adaptiver-Spiegel-\(Update: 05.05.2019\)](https://www.kugler-precision.com/index.php?Adaptiver-Spiegel-(Update:05.05.2019))
- SCANLAB GmbH, 2019; <https://www.scanlab.de/de/produkte/z-achsen-3d-erweiterungen/varioscan>, (Update: 04.05.2019)
- PI Ceramic GmbH, 2019; <https://www.piceramic.de/de/produkte/piezokeramische-aktoren/gestapelte-aktoren/p-010xxh-p-025xxh-pica-thru-ringaktoren-102800/>, (Update: 04.05.2019)
- Lemaitre, G. R. *Astronomical optics and elasticity theory: active optics methods*. Springer Science & Business Media, 2008 p. 171 ff